

# Light-controlled molecular tweezers capture specific amyloid oligomers

Chengyuan Qian<sup>1</sup>, Jiefang Chen<sup>1</sup>, Cheng Wang<sup>1</sup>, Qiang Wang<sup>1</sup>, Xiaoyong Wang<sup>2</sup>, and Xiaohui Wang<sup>1</sup>

<sup>1</sup>Nanjing Tech University

<sup>2</sup>Nanjing University

September 25, 2023

## Abstract

Amyloid- $\beta$  peptide ( $A\beta$ ) oligomers, characteristic symptom of Alzheimer's disease (AD), have been identified as the most neurotoxic species and significant contributors to neurodegeneration in AD. However, due to their transient and heterogeneous nature, the high-resolution structures and exact pathogenic processes of  $A\beta$  oligomers are currently unknown. Using light-controlled molecular tweezers (LMTs), we describe a method for precisely capturing specific  $A\beta$  oligomers produced from synthetic  $A\beta$  and AD animal models. Light irradiation can activate LMTs, which are composed of two  $A\beta$ -targeting pentapeptides (KLVFF) motifs and a rigid azobenzene (azo) derivative, to form a tweezer-like cis configuration that preferentially binds to specific oligomers matching the space of the tweezers via multivalent interactions of KLVFF motifs with the oligomers. Surprisingly, cis-LMTs can immobilize the captured oligomers in transgenic *Caenorhabditis elegans* (*C. elegans*) in vivo under light irradiation. The LMTs may serve as spatiotemporally controllable molecular tools to extract specific native oligomers for the structure and function studies via their reversible photoisomerization, which would improve the understanding of the toxic mechanisms of  $A\beta$  oligomers and development of oligomer-targeted diagnosis and therapy.

# Light-controlled molecular tweezers capture specific amyloid

## oligomers

Chengyuan Qian,<sup>1,2</sup> Jiefang Chen,<sup>1</sup> Cheng Wang,<sup>1</sup> Qiang Wang,<sup>1</sup> Xiaoyong Wang,<sup>\*2</sup>  
Xiaohui Wang<sup>\*1</sup>

<sup>1</sup>*Institute of Chemical Biology and Functional Molecules, State Key Laboratory of Materials-Oriented Chemical Engineering, School of Chemistry and Molecular Engineering, Nanjing Tech University, Nanjing 211816, P. R. China.*

<sup>2</sup>*State Key Laboratory of Pharmaceutical Biotechnology, School of Life Sciences, Nanjing University, Nanjing 210093, P. R. China.*

*\*Corresponding authors. E-mail address: wangxhui@njtech.edu.cn (Xiaohui Wang), boxwxy@nju.edu.cn (Xiaoyong Wang)*

### Abstract

Amyloid- $\beta$  peptide ( $A\beta$ ) oligomers, characteristic symptom of Alzheimer's disease (AD), have been identified as the most neurotoxic species and significant contributors to neurodegeneration in AD. However, due to their transient and heterogeneous nature, the high-resolution structures and exact pathogenic processes of  $A\beta$  oligomers are currently unknown. Using light-controlled molecular tweezers (LMTs), we describe a method for precisely capturing specific  $A\beta$  oligomers produced from synthetic  $A\beta$  and AD animal models. Light irradiation can activate LMTs, which are composed of two  $A\beta$ -targeting pentapeptides (KLVFF) motifs and a rigid azobenzene (azo) derivative, to form a tweezer-like *cis* configuration that preferentially binds to specific oligomers matching the space of the tweezers *via* multivalent interactions of KLVFF motifs with the oligomers. Surprisingly, *cis*-LMTs can immobilize the captured oligomers in transgenic *Caenorhabditis elegans* (*C. elegans*) *in vivo* under light irradiation. The LMTs may serve as spatiotemporally controllable molecular tools to extract specific native oligomers for the structure and function studies *via* their reversible photoisomerization, which would improve the understanding of the toxic mechanisms of  $A\beta$  oligomers and development of oligomer-targeted diagnosis and therapy.

**Keywords:** Amyloid oligomers; Precise capture; Molecular tweezers; Photoisomerization; Alzheimer's disease

### 1 Introduction

Protein misfolding and aggregation in the brain is a typical sign of a variety of neurodegenerative disorders.<sup>[1]</sup> The oligomeric aggregates of amyloid- $\beta$  peptides ( $A\beta$ ) are the principal neurotoxic species important to the onset of Alzheimer's disease (AD),<sup>[2,3]</sup> which is the most prevalent neurodegenerative illness associated with dementia.<sup>[4]</sup>  $A\beta$  oligomers not only cause various neuronal deficits in synaptic function, like loss of learning and memorial abilities,<sup>[5]</sup> but also activate other pathological processes of AD, such as tau hyperphosphorylation, oxidative stress, and mitochondrial dysfunction.<sup>[6]</sup> As a result,  $A\beta$  oligomers are recognized as legitimate targets for the diagnosis and therapy of AD.<sup>[7]</sup> Nevertheless, the term " $A\beta$  oligomer" is rather ambiguous because it refers to numerous soluble  $A\beta$  species or a combination of diverse types of metastable oligomeric species with varying sizes, shapes, and conformations as a result of  $A\beta$ 's dynamic assembly.<sup>[8]</sup> The structural changes may cause variances in the molecular toxicity of  $A\beta$  oligomers.<sup>[9]</sup> Therefore, accurate capture of the oligomers at the single aggregation level from  $A\beta$  mixtures is a critical step in elucidating the structural elements behind oligomer toxicity in AD pathological circumstances.

Due of the tremendous metastability and heterogeneity of  $A\beta$  oligomers, it is unfortunately very difficult to grasp a specific oligomer. Although significant effort has been made to date to identify  $A\beta$  oligomers using a variety of biosensors, including oligomer-specific antibodies,<sup>[10,11]</sup> small-molecule-based probes,<sup>[12-14]</sup> and electrochemical reporters<sup>[15,16]</sup> in combination with large-scale instruments, no one has been able to distinguish a particular oligomer at a degree of aggregation from the others in the mixture so far. Through covalent interactions, certain techniques have even been used to isolate specific oligomers from  $A\beta$  mixtures coupled with electrophoresis.<sup>[17-19]</sup> Such approaches, however, are unable to accurately represent the toxicity of naturally occurring oligomers since the captured oligomers may exhibit different cytotoxicity from that of the oligomers formed in self-aggregation due to differing structures.<sup>[20,21]</sup> Thus, new methods are urgently needed to capture and stabilize specific  $A\beta$  oligomers for the development of oligomer-targeted diagnosis and therapeutic strategies in anti-AD.

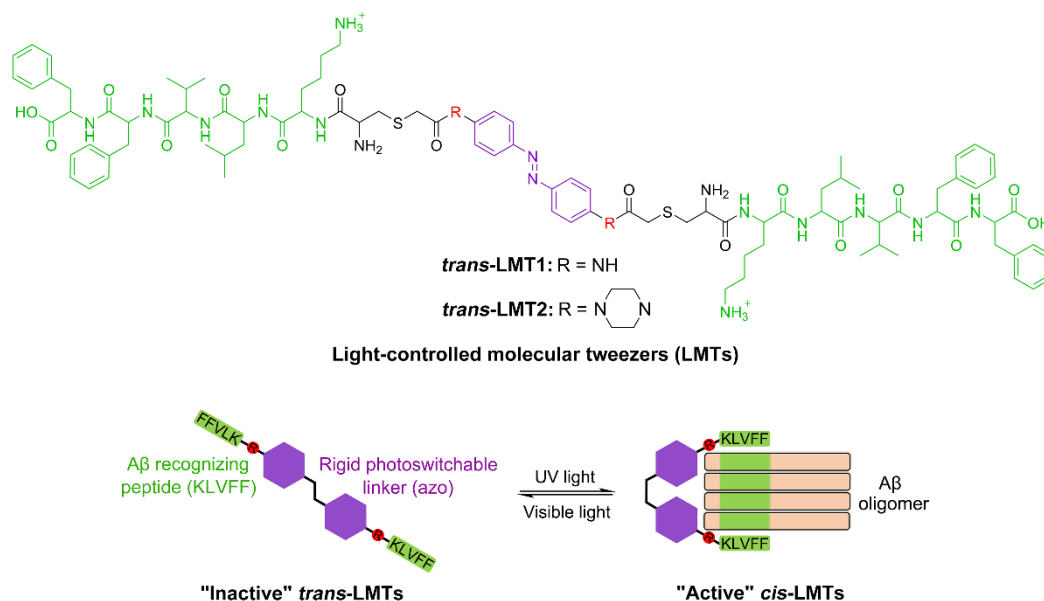


**Fig. 1.** Chemical structures of the LMTs and their mechanism for capturing specific A $\beta$  oligomers. The KLVFF is shown in green. The cartoon is not to scale because the whole architecture of A $\beta$  oligomers should be much bigger than that of azobenzene unit. For the sake of clarity, the phototransformation of azobenzene (azo) unit and the KLVFF motifs are highlighted.

To this aim, we present here the invention of light-controlled molecular tweezers (LMTs) to capture and stabilize the specific A $\beta$  oligomers by making use of the conformation features of A $\beta$  oligomers (Fig. 1). In general, A $\beta$  oligomers adopt solvent-exposed hydrophobic patches and antiparallel  $\beta$ -sheets. The region (KLVFF: residues 16–20) as the central hydrophobic core of A $\beta$  is responsible for A $\beta$  aggregation *via* self-interactions between neighboring strands (Fig. 1).<sup>[22]</sup> Accordingly, the pentapeptide KLVFF has been successfully employed to target A $\beta$  through interactions with the exposed KLVFF motif of A $\beta$  aggregates.<sup>[23]</sup> Small compounds containing photoresponsive groups, on the other hand, have demonstrated great promise for precise spatiotemporal manipulation of protein behavior and function, relying on their photoswitchable structures.<sup>[24-26]</sup> Notably, azobenzene (azo) is the most commonly utilized photochromic chemical in biomedical applications;<sup>[27,28]</sup> it undergoes *trans-cis* photoisomerization with significant geometrical alterations between planar *trans*- and non-planar *cis*-configurations. In this context, we created the LMTs by fusing the functions of KLVFF and azo groups. Through multivalent interactions of KLVFF motifs between the LMTs and oligomers, the LMTs are able to precisely “freeze” their chosen oligomers produced from both synthetic and natural A $\beta$  upon light irradiation. For the

first time, these LMTs provide a molecular technique to precisely capture individual A $\beta$  oligomers at a single aggregation level, which may remarkably advance studies on the structural and functional aspects of amyloid oligomers.

## 2. Results and discussion

### 2.1 Design and photoisomerization of LMTs

The two KLVFF motifs bridged by a flexible linker have been used to recognize low molecular weight (LMW) oligomers through binding to the KLVFF “ends” of A $\beta$  side chains.<sup>[29]</sup> However, the flexibility or length of the linker severely restricts the probe’s selectivity. For exact identification of a given A $\beta$  oligomer, rigid linkers that can adjust the distance between the two KLVFF motifs would be ideal. As a result, we chose azobenzene (azo) derivatives as stiff linker backbones for the LMTs. The distance between the phenyl termini ranges from 9.0 to 6.0 Å,<sup>[30]</sup> and this is likely to change the distance between the two KLVFF motifs when exposed to light. We believe that a convertible structure with suitable rigid substituents (R) *para* to the azo group will identify certain A $\beta$  oligomers (Fig. 1). Accordingly, because the compounds adopt tweezer-like configurations with relatively short distances between the two KLVFF motifs, *cis*-LMTs may be “active” to a specific A $\beta$  oligomer. As a result, a strong dual binding of KLVFF units of *cis*-LMTs to their “end” counterparts in the A $\beta$  oligomer with a matching size would occur. On the contrary, *trans*-LMTs may be “inactive” to specific A $\beta$  oligomers since they would adopt a single binding mode to A $\beta$  oligomers with low affinity due to the considerable distance between the two KLVFF motifs in such configurations. Thus, LMTs would offer light-controllable tools for capturing or isolating specific A $\beta$  oligomers with great spatiotemporal accuracy *via* a reversible transition between the *cis* and *trans* forms.

As a proof of concept, two models LMT1 and LMT2 were synthesized by reacting the iodoacetamide moiety of azo derivatives with the thiol of Cys residue in NH<sub>2</sub>-CKLVFF-COOH peptide. The synthetic route and characterization of the LMTs are described in the Supplementary Information. The photoisomerization of the LMTs was investigated by UV-Vis spectroscopy. As shown in Fig. 2A, the original *trans*-LMT1 displayed two characteristic bands at *ca.* 370 and 475 nm in Tris-HCl buffer, they are

$\pi$ - $\pi^*$  and  $n$ - $\pi^*$  absorptions of azo, respectively. Light irradiation at 365 nm led to a significant decrease of the strong  $\pi$ - $\pi^*$  transition and a slight increase of the  $n$ - $\pi^*$  band, which is typical of *trans*→*cis* isomerization of azo.<sup>[31]</sup> The photostationary state (PSS) of LMT1 was attained after continuous irradiation for 300 s (Fig. 2B), and it reached equilibrium with 66.7% of the *cis* form (Fig. S1). Within 30 s of further irradiation at 455 nm, the *cis* configuration was quickly changed back to the *trans* one (Fig. 2B). After 9 cycles of alternating between 365 and 455 nm, there was barely any loss of absorption (Fig. 2C). A complete recovery of *cis*-LMT1 to its *trans* form was achieved spontaneously by storing the solution at room temperature in the dark, with a half-life  $\tau_{1/2}$  of 1.26 h (Fig. S2). This time span is long enough for the binding of *cis*-LMT1 to an A $\beta$  oligomer. The optimized geometries of the LMTs isomers were calculated using the semiempirical quantum chemical method PM7. As anticipated, the conversion of the LMTs from the stretched planar *trans* configuration to the tweezer-like *cis* form dramatically reduces the distance between the KLVFF motifs (Fig. 2D and S3). Moreover, *cis*-LMT2 showed a greater separation between the KLVFF residues than *cis*-LMT1 due to the extension of azo group by piperazine at *para* positions. These findings suggest that the rigid “R” group and light irradiation can control the spacing between the KLVFF motifs.

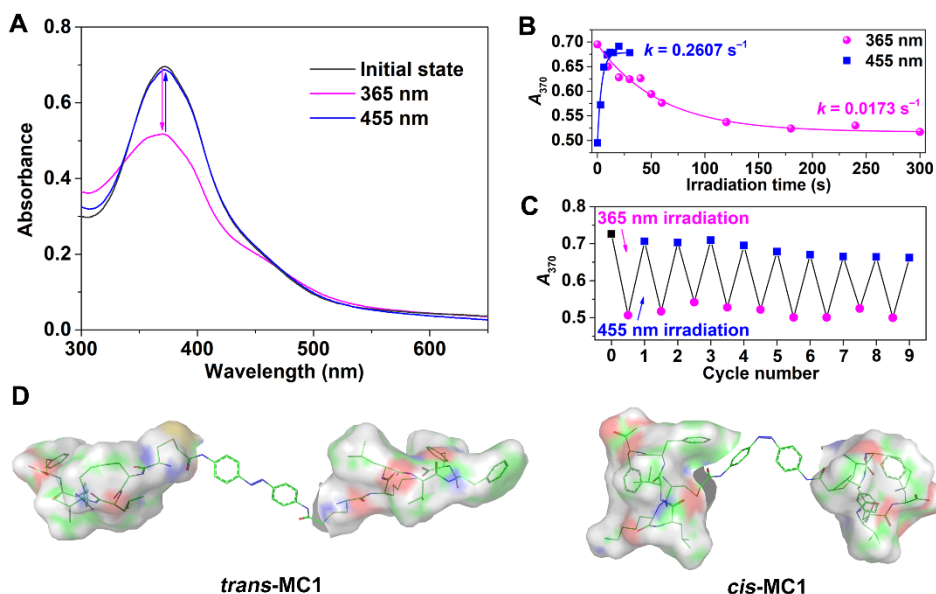


**Fig. 2.** (A) Absorption spectra of LMT1 before and after irradiation at 365 and 455 nm, respectively. (B) Photoisomerization kinetics of LMT1 monitored by UV-vis spectroscopy. (C) Reversible

conversion of LMT1 upon alternating irradiation at 365 and 455 nm, respectively. (D) Optimized geometries of *trans/cis*-LMT1 on calculations using the MOPAC2016 program package (version: 21.280).

## 2.2 *cis*-LMTs bind to specific oligomers of gel-separated A $\beta$

To test the light-driven binding of LMTs to synthetic A $\beta$  oligomers, native polyacrylamide gel electrophoresis (PAGE) was conducted, followed by a modified Western blotting. In the assay, biotin-labeled LMTs (LMTs-biotin) containing biotinylated KLVFF were used to investigate the binding properties of LMTs to A $\beta$  oligomers. KLVFF was biotinylated at C-terminal Lys (Fig. 3A). Briefly, the synthetic A $\beta$  mixture was initially separated by Tris-Tricine-PAGE.<sup>[32]</sup> LMTs-biotin was added to the membrane containing gel-transferred A $\beta$  species and co-incubated. Because the unbound LMTs-biotin can be easily washed away, only the adducts of LMTs-biotin with A $\beta$  were photographed on the membrane using streptavidin (SA)-conjugated horseradish peroxidase (HRP) solution with enhanced chemiluminescence (ECL). As a result of the very selective and stable interaction of SA with biotin, the bands of LMTs-biotin-preferred A $\beta$  oligomers can be observed on the membrane (Fig. 3B). In addition, standard Western blotting with anti-A $\beta$  antibody 6E10 confirmed the whole distribution of the A $\beta$  species on the membrane as a control.

Initially, the photoisomeric behaviors of LMTs-biotin were explored. LMT1-biotin exhibited almost the same spectral profile as LMT1 after irradiation at 365 and 455 nm (Fig. S4), demonstrating that the biotin groups had no impact on LMT1 isomerization. Because of the addition of piperazine groups, LMT2-biotin showed a spectacular red-shifted  $\pi$ - $\pi^*$  band at *ca.* 425 nm (Fig. S5).<sup>[33]</sup> It likewise exhibited sensitive and reversible photoisomerization between *trans* and *cis* configurations without degradation after 6 cycles of alternating low-power irradiation at 455 and 620 nm, respectively (Fig. S5D), although its thermal relaxation is faster than that of LMT1. Thus, utilizing LMTs-biotin, it is feasible to reveal the binding preference of LMTs to A $\beta$  oligomers.

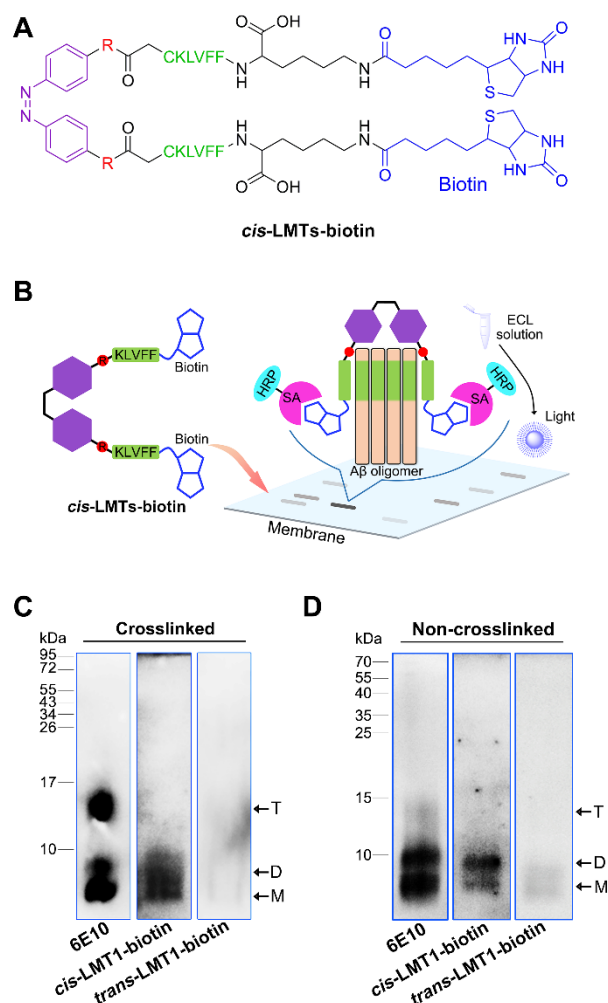


**Fig. 3.** (A) Chemical structure of *cis*-LMTs-biotin. (B) Schematic illustration of modified Western blotting for determining the preferred A $\beta$  oligomers of LMTs-biotin. Western blots of the LMT1-biotin-bound oligomers of crosslinked A $\beta$ 40 (C) and those of non-crosslinked A $\beta$ 40 (D). Anti-A $\beta$  antibody 6E10 was used as a control to indicate the distribution of A $\beta$ 40 species. M, D, and T stand for mono-, di-, and trimer, respectively. Same amounts of A $\beta$ 40 were loaded to each lane in the same set of experiments.

Given the metastability of A $\beta$  oligomers, we investigated the capacity of LMT1-biotin to bind stable synthetic A $\beta$  oligomers created by cross-linking unmodified A $\beta$  under irradiation.<sup>[17]</sup> The control group showed that A $\beta$ 40 included a significant number of monomers and trimers, but only a small amount of dimers (Fig. 3C). After imaging with SA-conjugated HRP, the bands of A $\beta$ 40 monomer and dimer were seen on the membrane that had been pre-treated with *cis*-LMT1-biotin (365 nm), but no trimer band was observed. *trans*-LMT1-biotin, on the other hand, did not show any bands. These results suggest that the dimer is the favored binding target for *cis*-LMT1 in the A $\beta$ 40 oligomers. Encouraged by the findings, we further studied the binding of LMT1-biotin

to the dynamic oligomers of A $\beta$ 40 without cross-linking pretreatment. In A $\beta$ 40 samples containing monomers, dimers, and a few of trimers, *cis*-LMT1-biotin (365 nm) still showed preferential binding to the dimers, as shown in Fig. 3D. *trans*-LMT1-biotin, on the other hand, scarcely bound to dimers, which is consistent with the binding to the crosslinked counterparts. The above findings show that *cis*-LMT1 can specifically capture A $\beta$  dimers in a light-driven manner, which is attributed to the appropriate distance between the two KLVFF units of *cis*-LMT1 for the two “end” KLVFF motifs of dimers, thereby forming stable adducts *via* multivalent KLVFF interactions. In contrast, *trans*-LMT1 was washed away from the membrane due to its low affinity for each A $\beta$  species through a single binding mode between KLVFF, resulting in the subtle bands. Because A $\beta$ 42 is more aggregation-prone than A $\beta$ 40,<sup>[12]</sup> the distribution of A $\beta$ 42 oligomers differed from that of A $\beta$ 40, with a high proportion of high molecular weight (HMW) oligomers in control groups. *cis*-LMT1-biotin (365 nm) still showed preferential binding to the dimers in both crosslinked and non-crosslinked A $\beta$ 42 samples (Fig. S6), confirming the selectivity of *cis*-LMT1 for A $\beta$  dimers.

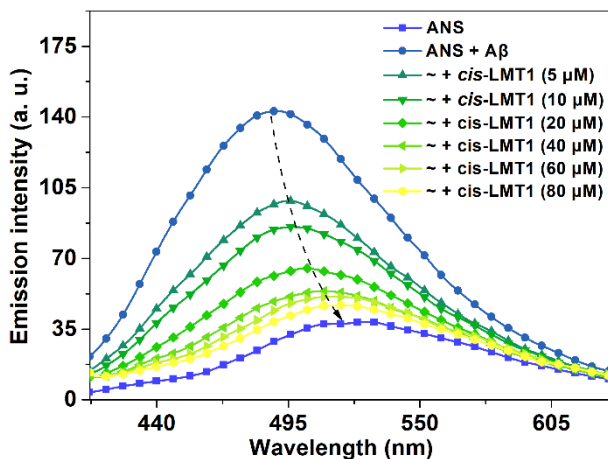


**Fig. 4.** Fluorescence spectra of ANS (20  $\mu$ M,  $\lambda_{\text{ex}}$  = 380 nm) in the absence and presence of A $\beta$ 40 with or without 5, 10, 20, 40, 60, and 80  $\mu$ M of *cis*-LMT1.

To validate the KLVFF-mediated binding mode of LMT1 to A $\beta$  oligomers, a fluorescence competition assay was performed using 8-anilinonaphthalene-1-sulfonate (ANS), which is a “turn-on” fluorescence probe for A $\beta$  oligomers through binding to the solvent-exposed hydrophobic patches of A $\beta$  oligomers, particularly the region of residues 16-22 (KLVFFAE),<sup>[34-36]</sup> As shown in Fig. 4, when 40  $\mu$ M (2 eq. of ANS) of

*cis*-LMT1 was added, the fluorescence of A $\beta$ -bound ANS was decreased and red-shifted to that of ANS *per se* suggesting that ANS was totally replaced by *cis*-LMT1. In contrast, the *cis* form of precursor 4,4'-bis(iodoacetamide)azobenzene (**2**) without KLVFF moieties cannot reduce the fluorescence of A $\beta$ -bound ANS (Fig. S7), consolidating that the binding of *cis*-LMT1 to A $\beta$  relies on the multivalent interactions of KLVFF motifs. Reasonably, such interactions at the region of KLVFF weakened A $\beta$ 's connection with ANS, leading to the detachment of the fluorescent probes from A $\beta$ .

Furthermore, the binding properties of LMT2-biotin to the crosslinked A $\beta$ 42 oligomers were evaluated to confirm the critical function of the distance between two KLVFF units of the tweezer-like structure in conformation-specific recognition of oligomers. Unlike *cis*-LMT1, which preferentially bound to A $\beta$  dimers, the increased distance between the two KLVFF motifs in *cis*-LMT2 allows for selective binding to oligomers bigger than dimers. As expected, *cis*-LMT2-biotin (455 nm) exhibited much higher binding selectivity to tetramers than to monomers and dimers (Fig. S8). There was no binding to the other A $\beta$ 42 species discovered. The results strongly support that *cis*-LMTs would provide a universal method for precise recognition of distinct A $\beta$  oligomers at the single aggregation level by altering the spacing between the two KLVFF motifs *via* modifying the rigid "R" groups *para* to the azo.

### 2.3 The *cis*-LMT1 captures dimers in synthetic A $\beta$ mixture

Encouraged by the binding preference of *cis*-LMT1 to A $\beta$  dimers, we next examined whether *cis*-LMT1 could capture the dimers in the A $\beta$  mixture using Western blotting with antibody 6E10. The aggregation profile of A $\beta$  monomers was measured by thioflavin (ThT) fluorescence in Tris buffer at 25 °C (Fig. S9).<sup>[37]</sup> Accordingly, A $\beta$  monomers were co-incubated with LMT1 for 6 h beyond the plateau phase, and 30 min irradiation was set at the lag phase from the beginning of incubation, the process for oligomers formation. After incubating A $\beta$ 40 *per se* for 6 h, only a minor number of LMW oligomers (~10 kDa) were seen on the membrane (Fig. 5A), indicating that the bulk of A $\beta$  would convert to be fibrils at this phase, consistent with the result of aggregation profile (Fig. S9). However, when A $\beta$ 40 was co-incubated with *cis*-LMT1,

an increase of oligomers (~10 kDa) assignable to the adducts of *cis*-LMT1 with A $\beta$ 40 dimers was detected (Fig. 5A). Moreover, 365 nm irradiation yielded a better impact than darkness. Contrarily, *trans*-LMT1 hardly affected the A $\beta$  aggregation. We believe that *cis*-LMT1 can capture the dimers and prevent them from further aggregation in the A $\beta$  mixture, which is probably attributed to the preferential binding of *cis*-LMT1 clamps to the dimers' two "end" KLVFF regions. Owing to the partial conversion to the "inactive" *trans* form *via* thermal relaxation during the co-incubation, treatment of A $\beta$  with *cis*-LMT1 thus yielded relatively fewer captured dimers in the dark for 6 h. Morphological examination using transmission electron microscopy (TEM) was also carried out to assess the effect of dimer-capturing of *cis*-LMT1 on A $\beta$  aggregation (Fig. 5B). A $\beta$  self-aggregation generated abundant fibrils, and *trans*-LMT1 had little effect on the fibrillary morphology. In the presence of *cis*-LMT1, tiny granules rather than fibrils were observed. Irradiation at 365 nm exhibited a greater inhibitory effect than darkness (Fig. 5B). In agreement with the results of Western blotting, A $\beta$  was frozen at a low aggregation degree by *cis*-LMT1 under irradiation, owing to *cis*-LMT1's capacity to capture and stabilize dimers.

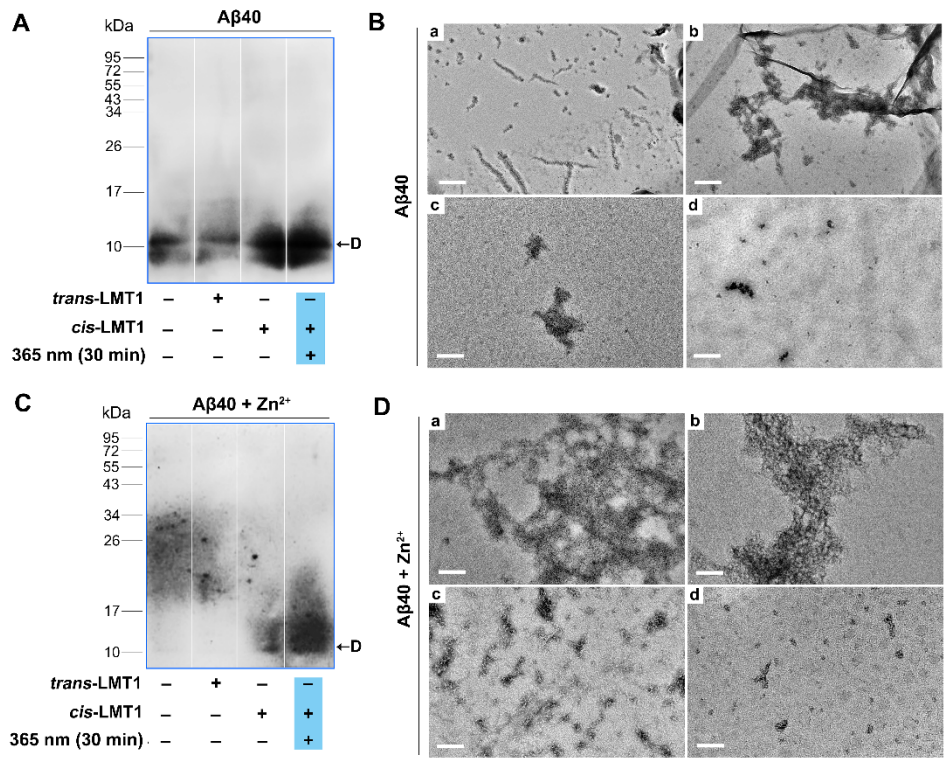


**Fig. 5.** (A) Western blot of the A $\beta$ 40 aggregates in the presence of *trans/cis*-LMT1 with or without irradiation at 365 nm for 30 min. (B) TEM images of A $\beta$ 40 aggregates in the presence of *trans/cis*-LMT1 with or without irradiation at 365 nm. a, A $\beta$ 40; b, A $\beta$ 40 + *trans*-LMT1; c, A $\beta$ 40 + *cis*-LMT1; d, A $\beta$ 40 + *cis*-LMT1 + 365 nm (30 min). (C) Western blot of the A $\beta$ 40 aggregates in the presence of Zn<sup>2+</sup> and *trans/cis*-LMT1 with or without irradiation at 365 nm for 30 min. (D) TEM images of Zn<sup>2+</sup>-induced A $\beta$ 40 aggregates in the presence of *trans/cis*-LMT1 with or without irradiation at 365 nm. a, A $\beta$ 40 + Zn<sup>2+</sup>; b, A $\beta$ 40 + Zn<sup>2+</sup> + *trans*-LMT1; c, A $\beta$ 40 + Zn<sup>2+</sup> + *cis*-LMT1; d, A $\beta$ 40 + Zn<sup>2+</sup> + *cis*-LMT1 + 365 nm (30 min). [A $\beta$ 40] = [LMTs] = [Zn<sup>2+</sup>] = 20  $\mu$ M. D stands for the adducts of *cis*-LMT1 with A $\beta$  dimer. Scale bars: 200 nm.

Considering that Zn<sup>2+</sup> can promote A $\beta$  aggregation, leading to greater heterogeneity of A $\beta$  mixture,<sup>[36]</sup> we also studied the effect of *cis*-LMT1 on the A $\beta$  dimers during Zn<sup>2+</sup>-induced A $\beta$  aggregation. Because Zn<sup>2+</sup> favored the formation of bulky aggregates,<sup>[38]</sup> no A $\beta$  oligomers were found in the presence of Zn<sup>2+</sup> after just 30 min (Fig. 5C). Interestingly, *cis*-LMT1 can create considerable quantities of LMW oligomers (~10 kDa) when exposed to 365 nm light for 30 min (Fig. 5C). On the contrary, *trans*-LMT1 was almost ineffective to stabilize A $\beta$  dimers. TEM assay manifested that only the *cis*-LMT1-treated group could clearly suppress Zn<sup>2+</sup>-induced A $\beta$  aggregation by producing tiny aggregates under irradiation (Fig. 5D). These findings suggest that *cis*-LMT1 is able to freeze the A $\beta$  dimers in the mixture of Zn<sup>2+</sup>-induced A $\beta$  aggregates. Although the PSS of LMT1 has a limited number of *cis*-isomers, continual irradiation created new *cis*-LMT1 as the original *cis*-LMT1 was consumed, ensuring effective dimer binding. Therefore, by sequestering the dimers in its clamps, *cis*-LMT1 might serve as an effective light-driven capture for synthetic A $\beta$  dimers.

Intervening A $\beta$  aggregation may alter the A $\beta$ -induced neurotoxicity. Using the MTT assay, we thus tested the ability of *cis*-LMT1 to capture dimers and its effect on A $\beta$ -induced neurotoxicity in PC12 cells. LMT1 *per se* was nontoxic even the concentration was up to 40  $\mu$ M (Fig. 6A). After a 24-hour co-incubation in the dark, A $\beta$ 42 self-aggregation decreased the cell viability to ~80%, due to the neurotoxicity of aggregates. While the cell viability was recovered to ~86% in the presence of *cis*-LMT1 (Fig. 6B), probably resulting from its inhibitory effect on A $\beta$  aggregation. In contrast, *trans*-LMT1 cannot influence the A $\beta$ -induced cytotoxicity due to its inability to interfere with A $\beta$  aggregation. Given the toxicity of oligomers, the limited inhibitory effect of *cis*-LMT1 on A $\beta$ -induced neurotoxicity is very likely attributed to the dimer stabilization

that would make the A $\beta$  staying at LMW oligomeric states, although the binding of *cis*-LMT1 to dimers may reduce their toxicity to some extent. These results imply that *cis*-LMT1 can also freeze A $\beta$  dimers and prevent A $\beta$  aggregation in living cells.

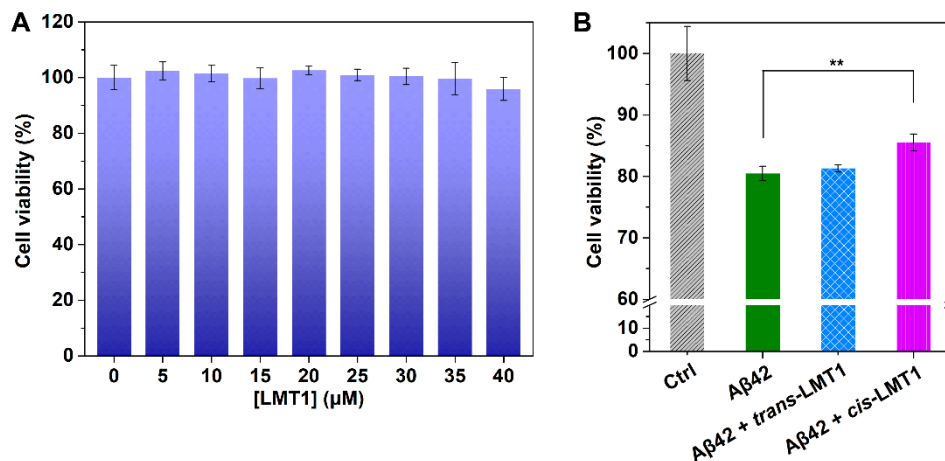


**Fig. 6.** (A) Viability (%) of PC12 cells after incubation with different concentrations of LMT1 for 24 h. Effects of *trans/cis*-LMT1 (20 μM) on viability of PC12 cells in the presence of A $\beta$ 42 (20 μM) upon co-incubation for 24 h. Data was normalized and calculated as a percentage of untreated cells only containing 1% DMSO as a control. Error bars indicate  $\pm$  S.D. ( $n = 3$  independent experiments). \* $P < 0.01$  (Student's  $t$ -test).

#### 2.4 The *cis*-LMT1 captures natural A $\beta$ dimers in *C. elegans*

Inspired by the light-driven action of *cis*-LMT1 on synthetic A $\beta$  dimers, we further investigated its effect on natural A $\beta$ 42 in the AD model—transgenic *Caenorhabditis elegans* (*C. elegans*). *C. elegans* strain CL4176 expresses A $\beta$ 42 in the body wall muscle cells; higher temperature (25 °C) can stimulate A $\beta$ 42 aggregation, resulting in toxic aggregates in the worms and a progressive paralysis.<sup>[39,40]</sup> To determine whether *cis*-LMT1 could capture natural A $\beta$  dimers in *C. elegans*, Western blotting assay was carried out to examine the distribution of A $\beta$  in the worms following the treatment of LMT1 with or without irradiation at 365 nm for 8 h. As shown in Fig. 7A, no bands of LMW oligomers were seen in either the vehicle or *trans*-MC1 groups, most likely due to the massive aggregation of A $\beta$ 42. Notably, *cis*-LMT1-treated group clearly showed the adducts of *cis*-LMT1 with A $\beta$ 42 dimer at a band (~10 kDa) and other LMW species under irradiation. These results signify that *cis*-LMT1 is still effective for capturing natural A $\beta$  dimers *in vivo*.

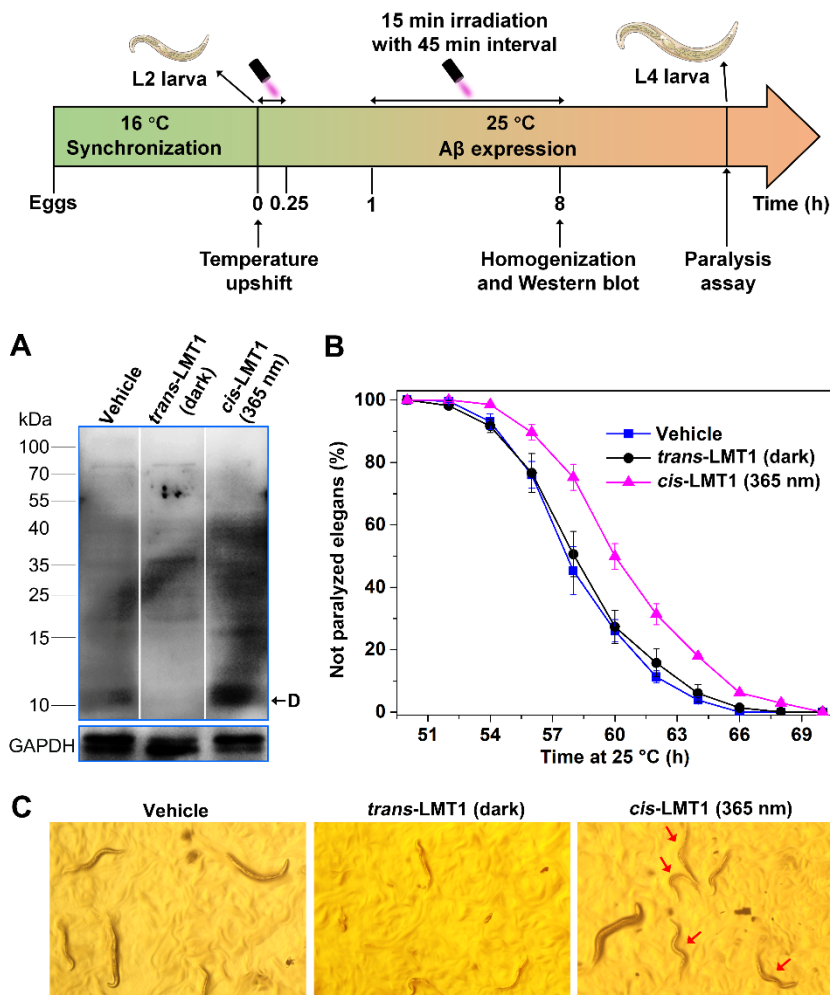


**Fig. 7.** Top: Scheme of transgenic *C. elegans* experiments for determining the dimer-capturing properties of LMTs. Bottom: (A) Western blots of Aβ42 extracted from *C. elegans* strain CL4176 treated with or without *trans*-LMT1 (10 μM) in the dark or *trans*-LMT1 (10 μM) under light irradiation at 365 nm. D stands for the adducts of LMT1 and Aβ42 dimer. (B) Effects of LMT1 (10 μM) on the Aβ42-induced paralysis in transgenic *C. elegans* strain CL4176 with or without irradiation at 365 nm. (C) Motion modes of *C. elegans* strain CL4176 treated with or without *trans*-LMT1 (10 μM) in the dark or *trans*-LMT1 (10 μM) under light irradiation at 365 nm after feeding at 25 °C for 60 h. Data are mean ± standard deviation ( $n = 3$ ). Red arrows indicate the unparalyzed worms.

The worm paralysis experiment can reflect the influence of dimer-capturing of *cis*-LMT1 on Aβ neurotoxicity *in vivo*. The Aβ-induced paralysis was monitored after the temperature was upshifted to 25 °C, which was hardly affected by light irradiation (Fig. S10). Compared to the vehicle group, treatment with *cis*-LMT1 and irradiation at 365 nm obviously postponed the paralysis (Fig. 7B), suggesting that *cis*-LMT1 could alleviate the neurotoxicity of Aβ aggregation in *C. elegans* by blocking the aggregation *via* freezing Aβ42 dimers. In the dark, there was almost no delay in paralysis in worms treated with *trans*-LMT1, confirming that *trans*-LMT1 cannot intervene Aβ

aggregation *in vivo*. The effects of LMT1 on paralysis were certified by the motion mode of the CL4176 *elegans* at 60 h post-temperature shift to 25 °C (Fig. 7C and Movie S1-S3). The majority of the worm bodies stiffened in both the vehicle and *trans*-LMT1-treated groups, with just the heads moving slowly; however, when exposed to light (365 nm), the *cis*-LMT1-treated worms wriggled fast with curvy bodies. These results demonstrate that *cis*-LMT1 can also capture and stabilize the A $\beta$ 42 dimers in *C. elegans*, thereby inhibiting A $\beta$  aggregation and attenuating toxicity. It should be pointed out that similar with the result of cytotoxicity assay, the amelioration of A $\beta$ -induced neurotoxicity seems not good enough for therapeutic purpose, because of the generation of toxic LMW A $\beta$  oligomers resulting from the capture and stabilization of *cis*-LMT1 to dimers. Although we believe that LMTs are promising candidates to construct the targeting scavengers for oligomers to effectively reduce A $\beta$ -induced neurotoxicity. However, this hypothesis needs a separate investigation, which would be out of the scope of the present study.

### 3 Conclusions

For the first time, we developed light-controlled molecular tweezers (LMTs) for the precise capture of specific A $\beta$  oligomers. The LMTs were constructed by bridging two KLVFF motifs to the rigid photoswitchable azobenzene core. The distance between two KLVFF motifs could be varied by photoisomerization of azobenzene at different wavelengths, allowing tweezer-like *cis*-LMTs capable of seizing the two “end” KLVFF sequences in A $\beta$  oligomers. The selectivity of *cis*-LMTs for specific A $\beta$  oligomers was achieved by tuning the space between the clamp arms using substituents of azobenzene at *para* positions. Once the *cis*-LMTs possess a suitable room to accommodate the specific A $\beta$  oligomers, they preferentially capture the oligomers *via* multivalent interactions between KLVFF motifs. As a proof of concept, *cis*-LMT1 successfully captures dimers of both synthetic and natural A $\beta$  from mixture *in vitro* and *in vivo* under light irradiation. Moreover, this binding mechanism allows the *cis*-LMT1 to stabilize captured dimers in neuron cells and AD worms. Given the structure’s considerable tunability, the molecular tweezers presented here may offer a universal molecular platform to build a toolbox for specific amyloid oligomers in a variety of contexts.

Based on the reversible photoisomerization, LMTs would be promising starting scaffolds to achieve extraction or elimination of specific natural A $\beta$  oligomers for studying the pathogenesis and structures of oligomers and developing oligomer-targeted therapy of AD.

### Acknowledgements

We appreciate the financial support from the National Natural Science Foundation of China (Grants 21771105, 21877059), the Natural Science Foundation of Jiangsu Province (Grant BK20170103), and the Six Talent Peaks Project in Jiangsu Province (Grant SWYY-043).

### Conflict of interest

The authors declare no competing financial interests.

### References

1. C. Soto, S. Pritzkow, *Nat. Neurosci.* **2018**, *21*, 1332.
2. I. Benilova, E. Karran, B. De Strooper, *Nat. Neurosci.* **2012**, *15*, 349.
3. R. Nortley, N. Korte, *Science* **2019**, *365*, eaav9518.
4. D. J. Selkoe, *Science* **2012**, *337*, 1488.
5. C. Haass, D. J. Selkoe, *Nat. Rev. Mol. Cell Biol.* **2007**, *8*, 101.
6. S. J. Lee, E. Nam, H. J. Lee, M. G. Savelieff, M. H. Lim, *Chem. Soc. Rev.* **2017**, *46*, 310.
7. E. Karran, B. De Strooper, *Nat. Rev. Drug Discovery* **2022**, *21*, 306.
8. Y. Wang, J. Chen, F. Gao, M. Hu, X. Wang, *Org. Biomol. Chem.* **2023**, *21*, 4540.
9. S. De, D. C. Wirthensohn, P. Flagmeier, *Nat. Commun.* **2019**, *10*, 1541.
10. K. Kulenkampff, A. -M. Wolf Perez, P. Sormanni, J. Habchi, M. Vendruscolo, *Nat. Rev. Chem.* **2021**, *5*, 277.
11. F. A. Aprile, P. Sormanni, M. Podpolny, S. Chhangur, L. -M. Needham, F. S. Ruggeri, M. Perni, R. Limbocker, G. T. Heller, T. Sneideris, T. Scheidt, B. Mannini, J. Habchi, S. F. Lee, P. C. Salinas, T. P. J. Knowles, C. M. Dobson, M. Vendruscolo, *Proc. Natl. Acad. Sci. U. S. A.* **2020**, *117*, 13509.
12. Y. Zhang, C. Ding, C. Li, X. Wang, *Adv. Clin. Chem.* **2021**, *103*, 135.
13. M. Habashi, S. Vutla, K. Tripathi, S. Senapati, P. S. Chauhan, A. Haviv-Chesner, M. Richman, S. A. Mohand, V. Dumulon-Perreault, R. Mulamreddy, E. Okun, J. H. Chill, B. Guerin, W. D. Lubell, S. Rahimpour, *Proc. Natl. Acad. Sci. U. S. A.* **2022**, *119*, e2210766119.
14. M. Rodrigues, P. Bhattacharjee, A. Brinkmalm, D. Do, C. Pearson, S. De, A. Ponjavic, J. Varela, K. Kulenkampff, I. Baudrexel, *Nat. Chem.* **2022**, *14*, 1045.
15. Y. Zhou, L. Liu, Y. Hao, M. Xu, *Chem. Asian J.* **2016**, *11*, 805.
16. J. Qin, D. G. Jo, M. Cho, Y. Lee, *Biosens. Bioelectron.* **2018**, *113*, 82.
17. G. Bitan, D. B. Teplow, *Acc. Chem. Res.* **2004**, *37*, 357.
18. G. M. Shankar, S. Li, T. H. Mehta, A. Garcia-Munoz, N. E. Shepardson, I. Smith, F. M. Brett, M. A. Farrell, M. J. Rowan, C. A. Lemere, C. M. Regan, D. M. Walsh, B. L. Sabatini, D. J. Selkoe, *Nat. Med.* **2008**, *14*, 837.
19. M. Jin, N. Shepardson, T. Yang, G. Chen, D. Walsh, D. J. Selkoe, *Proc. Natl. Acad. Sci. U. S. A.*

- 2011, 108, 5819.
20. E. E. Cawood, N. Guthertz, J. S. Ebo, *J. Am. Chem. Soc.* 2020, 142, 20845.
21. N. Gao, Z. Liu, H. Zhang, C. Liu, D. Yu, J. Ren, X. Qu, *Angew. Chem. Int. Ed.* **2022**, 61, e202115336.
22. M. Ahmed, J. Davis, D. Aucoin, T. Sato, S. Ahuja, S. Aimoto, J. I. Elliott, W. E. Van Nostrand, S. O. Smith, *Nat. Struct. Mol. Biol.* **2010**, 17, 561.
23. M. Ma, Z. Liu, N. Gao, Z. Pi, X. Du, J. Ren, X. Qu, *J. Am. Chem. Soc.* **2020**, 142, 21702.
24. K. Hüll, J. Morstein, D. Trauner, *Chem. Rev.* **2018**, 118, 10710.
25. P. Paoletti, G. C. R. Ellis-Davies, *Nat. Rev. Neurosci.* **2019**, 20, 514.
26. H. Gerwe, F. He, *Angew. Chem. Int. Ed.* **2022**, 61, e202203034.
27. A. A. Beharry, G. A. Woolley, *Chem. Soc. Rev.* **2011**, 40, 4422.
28. F. A. Jerca, V. V. Jerca, R. Hoogenboom, *Nat. Rev. Chem.* **2022**, 6, 51.
29. A. A. Reinke, P. M. Ung, J. J. Quintero, H. A. Carlson, J. E. Gestwicki, *J. Am. Chem. Soc.* **2010**, 132, 17655.
30. R. Göstl, A. Senf, S. Hecht, *Chem. Soc. Rev.* **2014**, 43, 1982.
31. H. M. Bandara, S. C. Burdette, *Chem. Soc. Rev.* **2012**, 41, 1809.
32. H. Schägger, *Nat. Protoc.* **2006**, 1, 16.
33. S. Samanta, A. Babalhavaeji, M. X. Dong, G. A. Woolley, *Angew. Chem. Int. Ed.* **2013**, 52, 14127.
34. A. R. Ladiwala, J. Litt, R. S. Kane, D. S. Aucoin, S. O. Smith, S. Ranjan, J. Davis, W. E. Van Nostrand, P. M. Tessier, *J. Biol. Chem.* **2012**, 287, 24765.
35. R. Limbocker, S. Chia, F. S. Ruggeri, M. Perni, R. Cascella, G. T. Heller, G. Meisl, B. Mannini, J. Habchi, T. C. T. Michaels, P. K. Challa, M. Ahn, S. T. Casford, N. Fernando, C. K. Xu, N. D. Kloss, S. I. A. Cohen, J. R. Kumita, C. Cecchi, M. Zasloff, S. Linse, T. P. J. Knowles, F. Chiti, M. Vendruscolo, C. M. Dobson, *Nat. Commun.* **2019**, 10, 225.
36. H. Liu, C. Qian, T. Yang, Y. Wang, J. Luo, C. Zhang, X. Wang, X. Wang, Z. Guo, *Chem. Sci.* **2020**, 11, 7158.
37. C. Ding, C. Li, Q. Meng, C. Qian, C. Zhang, L. Yang, X. Wang, Y. Wang, *Sensors Actuators B: Chem.* **2021**, 347, 130607.
38. X. Wang, X. Wang, Z. Guo, *Coord. Chem. Rev.* **2018**, 362, 72.
39. B. Zott, M. M. Simon, *Science* **2019**, 365, 559.
40. C. D. Link, *Proc. Natl. Acad. Sci. U. S. A.* **1995**, 92, 9368.